Establishing an experimental rat model of photo-dynamically-induced retinal vein occlusion using erythrosin B

Wei Chen[1], Ying Wu[1], Mi Zheng[1], Qing Gu[1], Zhi Zheng[1], Xin Xia[1,2]

[1]Department of Ophthalmology, Shanghai First People's Hospital, School of Medicine, Shanghai Jiaotong University, Shanghai 200080, China

[2]Shanghai Key Laboratory of Fundus Diseases, Shanghai Jiaotong University, Shanghai 200080, China

Correspondence to: Xin Xia. Department of Ophthalmology, Shanghai First People's Hospital, School of Medicine, Shanghai Jiaotong University, No.100 Haining Road, Shanghai 200080, China. xiaxin05@gmail.com

Abstract

• **AIM:** To develop a reliable, reproducible rat model of retinal vein occlusion (RVO) with a novel photosensitizer (erythrosin B) and study the cellular responses in the retina.

• **METHODS:** Central and branch RVOs were created in adult male rats *via* photochemically-induced ischemia. Retinal changes were monitored *via* color fundus photography and fluorescein angiography at 1 and 3h, and 1, 4, 7, 14, and 21d after irradiation. Tissue slices were evaluated histopathologically. Retinal ganglion cell survival at different times after RVO induction was quantified by nuclear density count. Retinal thickness was also observed.

• **RESULTS:** For all rats in both the central and branch RVO groups, blood flow ceased immediately after laser irradiation and retinal edema was evident at one hour. The retinal detachment rate was 100% at 3h and developed into bullous retinal detachment within 24h. Retinal hemorrhages were not observed until 24h. Clearance of the occluded veins at 7d was observed by fluorescein angiography. Disease manifestation in the central RVO eyes was more severe than in the branch RVO group. A remarkable reduction in the ganglion cell count and retinal thickness was observed in the central RVO group by 21d, whereas moderate changes occurred in the branch RVO group.

• **CONCLUSION:** Rat RVO created by photochemically-induced ischemia using erythrosin B is a reproducible and reliable animal model for mimicking the key features of human RVO. However, considering the 100% rate of retinal detachment, this animal model is more suitable for studying RVO with chronic retinal detachment.

• **KEYWORDS:** retinal vein occlusion; ischemia; laser photothrombosis; rat model

INTRODUCTION

Retinal vein occlusion (RVO), whether central retinal vein occlusion (CRVO) or branch retinal vein occlusion (BRVO), is the second most common retinal vascular disease after diabetic retinopathy [1]. Pooled data from population studies conducted in the United States, Europe, Asia, and Australia suggest that RVO affects about 16 million adults [2]. Unfortunately, there is currently no definitive treatment for RVO. Recently reported treatments that involve direct intravitreal injections of anti-vascular endothelial growth factor (VEGF) agents may improve best corrected visual acuity, but serious adverse side effects such as cataract and elevation of intraocular pressure cannot be ignored. A reliable animal model of RVO (CRVO and BRVO) is still needed in pharmacotherapy research.

Several methods for inducing RVO in rabbits, cats, or rats have been described, including light coagulation, endothelin-1 injection, mechanical ligation, and photodynamic thrombosis [3-7]. Currently, the most common method to induce RVO in rats is laser photocoagulation with a photosensitizer [7]. The photosensitizer in RVO animal models is usually rose bengal, and the laser energy required to activate rose bengal is high. Thus it is worth studying whether another photosensitizer that requires less energy can be applied to develop a laser-induced photothrombotic model of RVO.

Erythrosin B is an artificial dye widely used in the food and textile industries. It has a high molar absorption coefficient and singlet oxygen quantum yield, which makes it a potential photosensitizer for photodynamic applications. Erythrosin B irradiated by laser has been used to develop animal models of posterior ischemic optic neuropathy, neuropathic pain, and

distal middle cerebral artery occlusion [8-10]. This laser-driven photochemical technique causes direct peroxidation of the endothelial membrane by singlet molecular oxygen, then this photochemically-induced endothelial damage specifically attracts platelets, and then platelets degranulate and self-sensitize a chain process of aggregation, which leads to vascular occlusion.

Current data is incomplete with regard to the natural history of CRVO or BRVO in the rat model, notably at the cellular level. In the present study, we developed a rat model of RVO using erythrosin B as a photosensitizer and characterized it through fundus photography, fluorescein angiography, and histological analysis. Our objective in the present study was to demonstrate the potential usefulness and practicality of this rat model for studying obstructive changes in the retinal vasculature in RVO. Our present review of the course of RVO using this model could help other investigators decide whether this is an appropriate model for their specific interventions.

MATERIALS AND METHODS

Animals Twenty-six (13 CRVO and 13 BRVO) adult male Sprague-Dawley rats (weight 250-350 g) were used in this study. All procedures concerning animals were performed in accordance with the ARVO Statement for the Use of Animals in Ophthalmic and Vision Research. Prior to examination or treatment, all rats were anesthetized by intraperitoneal injection of ketamine hydrochloride (100 mg/kg body weight). Eyes were topically anesthetized with oxybuprocaine hydrochloride eye drops and the pupils were dilated with 1% tropicamide solution prior to laser application.

Creation of Central Retinal Vein Occlusion or Branch Retinal Vein Occlusion In all animals, RVO was created using a 532-nm green laser (Coherent Novus Omni, America) mounted on a slit lamp. Only the right eye of each animal was used; the fellow eye served as a contralateral control. Each animal was positioned facing the slit-lamp laser delivery system, with one eye lighted touching a fixed glass cover slip, so that details of the fundus could be visualized through the biomicroscope. Erythrosin B (2%) was injected via the superficial dorsal vein of the penis at a dose of 20 mg/kg. Within 3min the laser was applied to the selected retinal veins. The irradiated spot was 1.5-2.0 optic disk diameters away from the optic nerve. Laser parameter settings were: 100 μm in diameter, 0.2s exposure time, and 100 mW of power. Five to ten shots were applied to each spot before the blockage was observed. All major veins were occluded in CRVO models, while only the nasal three veins were occluded in the BRVO procedure to generate a nasal hemi-retinal occlusion. During irradiation, the temperature of the rats was maintained at 37-38℃.

Retinal Photography and Fluorescein Angiography Fundus color photography and angiography were performed at 1 and 3h, and 1, 2, 4, 7, 14, and 21d after treatment to observe the evolution of venous occlusion and related retinal response. Eyes covered with a fixed glass cover slip were placed under a stereomicroscope and the fundus was recorded by a digital camera (Canon 90D, Japan). Fluorescein sodium solution (10%, 0.2 mL) was intravenously injected, and penetration into the eyes was confirmed by the yellow change in color of the conjunctiva, at which time angiographs were recorded (Heidelberg HRT2, Germany).

Histopathological Analysis Retinal histological changes were examined 7, 14, and 21d after laser treatment. Four rats at each timepoint and group were euthanized by an anesthetic overdose for histopathologic examination. The eyes were enucleated immediately under a stereomicroscope and immersed in 4% paraformaldehyde for 24h at 40℃ prior to paraffin embedding. In the BRVO model, to mark the venous occlusion side a suture was performed at the nasal side prior to enucleating. Sections 5-μm thick obtained by a microtome were stained with hematoxylin and eosin and examined by light microscopy.

To compare the differences in histological reaction between the laser-treated and contralateral control eyes, cells in the ganglion cell layer (GCL) were counted to evaluate cell loss in two retinal areas (peripheral and para-optic nerve). For the BRVO group, the untreated temporal side of the retina of the same eye also served as a control. The number of nuclei in targeted areas of the GCL of the posterior pole (500 μm from the center of the optic disc) and the peripheral retina (4 mm from the center of the optic disc) were taken with an eyepiece reticule of a microscope at 400 × magnification. Counts were taken from a comparable area on three consecutive slides by two independent individuals (one was unaware of the treatment). The average number of cells in peripheral-, para-optic nerve-, and whole- retina sections (combining peripheral and para-optic cell counts) was calculated. The percent cell loss was calculated as: (control cells-treated cells) /control cells ×100%.

Statistical Analysis Analysis of variance (ANOVA), Student's *t*-test and Chi-squared tests were used to compare differences in the effects of the laser-applied RVO models, time points, and retinal regions.

RESULTS

Color Fundus Photography and Fluorescein Angiography Two rats (8%) were excluded from further study because the vessel wall was ruptured during the laser application which resulted in a vitreous hemorrhage over the laser site. The rest of the rats all successfully developed RVO.

In the CRVO group immediately after laser irradiation, there was no blood flow in the retinal veins or the flow was extremely slow. The coagulated sites showed extreme
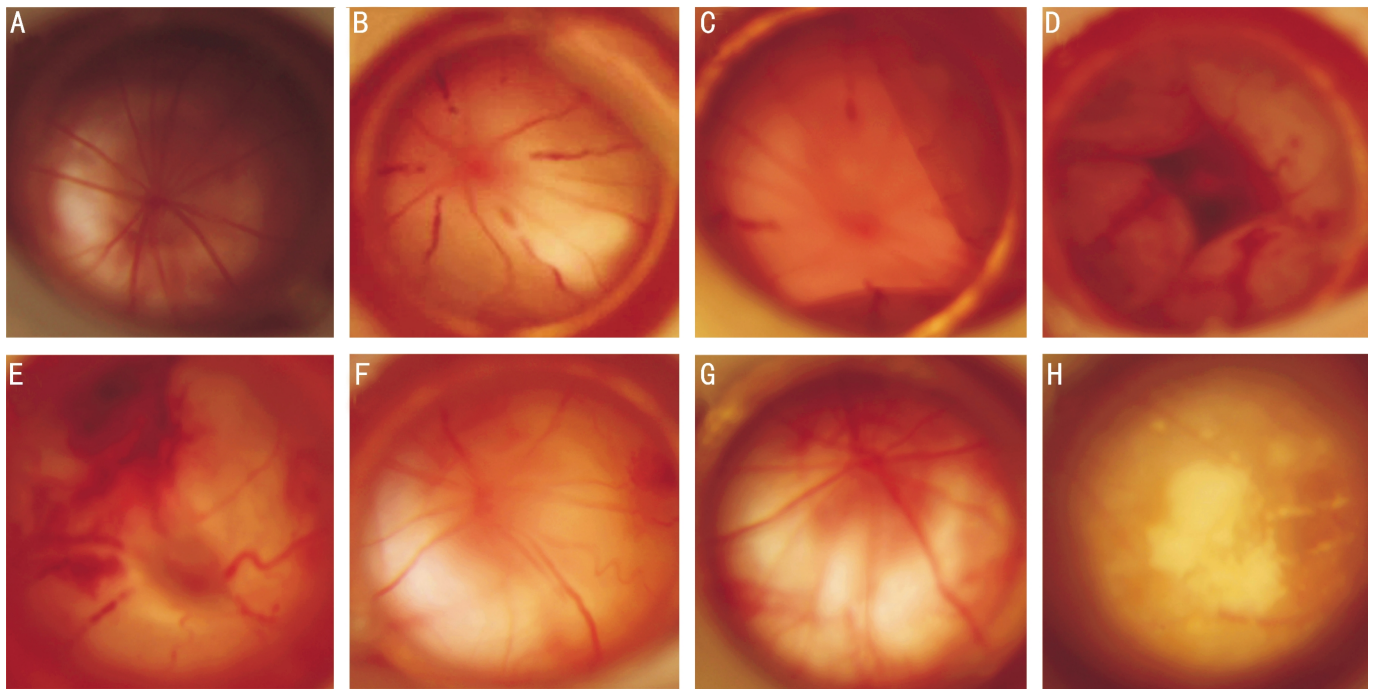
Figure 1 Representative fundus photographs of a CRVO rat before and at each timepoint after laser irradiation A: Normal rat retina before irradiation; B: At 1h after irradiation the retinal veins were occluded and dilated, and the retina became edematous; C: At 3h, peripheral RD; D: After 1d, bullous RD and disseminated retinal hemorrhages emerged; E: At 4d, RD partially resolved; F: By 7d, the retina reattached spontaneously with a reduced number of peripheral hemorrhages; G: At 14d, the affected retina appeared pale; H: By 21d, yellow precipitates were occasionally observed.
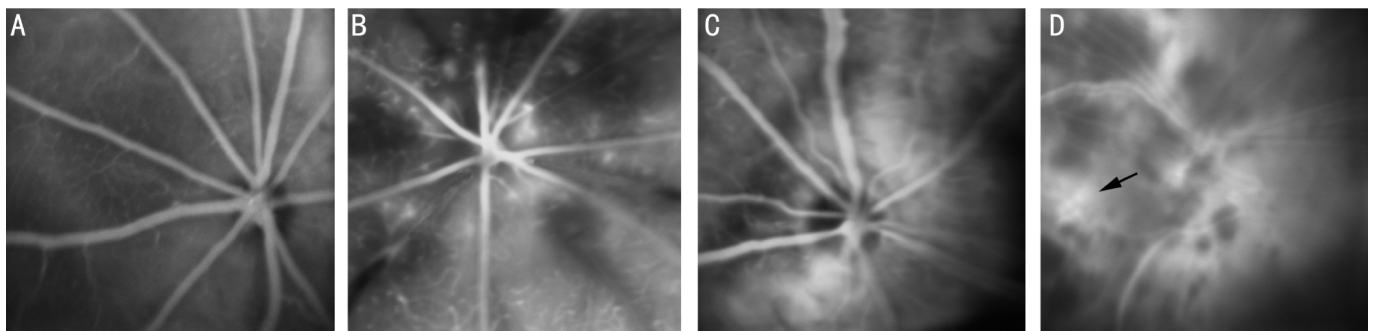
Figure 2 Representative fluorescein angiographys of rat CRVO retina at different timepoints A: Normal rat retina; B: One hour post-irradiation, complete retinal vein occlusion and leakage can be seen from both the laser-occluded sites and capillaries surrounding the coagulated tissue; C: At 7d, fluorescein angiography revealed reopening of the occluded veins and tortuous arteries and veins; D: At 21d, in rats with yellow precipitates focal retinal hyperfluorescence (black arrow) was occasionally observed, indicating neovascular tufts.

vascular constriction and the distal veins appeared dilated and tortuous (Figure 1). Extensive retinal edema was evident 1h after laser treatment and resulted in peripheral retinal detachment (RD) at 3h. The periphery RD developed to a significant bullous RD within 24h. Superficial and deep retinal hemorrhages were not observed until 1d after treatment. Retinal edema and hemorrhage steadily increased until 4d, at which time they began to gradually subside. Slit lamp examination at 7d suggested that the detached retina had reattached spontaneously and regained a transparent appearance, with a reduced number of peripheral hemorrhages. The affected retina appeared pale after 14d, and by 21d yellow precipitates were occasionally observed. Fluorescein angiography revealed complete retinal venous occlusion 1h after laser irradiation, with marked fluorescein

leakage from both laser-occluded sites and capillaries surrounding the area of the coagulated tissue (Figure 2). Seven days after laser irradiation, reopening of the occluded veins and tortuous arteries and veins were observed on fluorescein angiography. In rats with yellow precipitates, focal retinal hyperfluorescence was occasionally observed at 21d, an indication of neovascular tufts.

In the BRVO group, the progression of RVO was similar to that of the CRVO group (Figure 3). Hemiretinal vein occlusion was seen immediately after laser treatment, followed by venous dilatation and tortuosity of the entire retinal vessels. After 1h, the retina appeared edematous, with an outstanding change on the treated side. On the occluded side, RD could be observed at 3h, starting from the periphery of the retina and spreading across the entire retina within
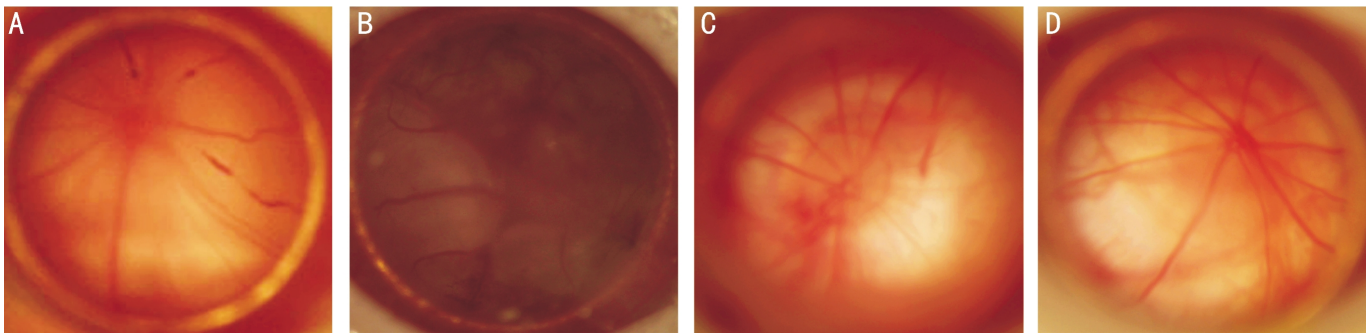
Figure 3 Representative fundus photographs of rat BRVO at different timepoints A: Although only three retinal veins on the nasal side were occluded, the entire retina became edematous at 1h post-irradiation; B: After 1d, bullous RD and disseminated retinal hemorrhages formed; C: After 7d, while the entire retina looked pale, this was especially so on the treated side; D: Edema and hemorrhage disappeared by 14d.

24h. However, retinal hemorrhages were only observed on the occluded side until 24h after laser treatment. Edema and hemorrhage peaked at 4d, gradually decreased by 7d, and eventually disappeared by 14d.

Pathological Changes Between the CRVO eyes and the untreated control eyes, there were significant declines in the densities of nuclei in the GCL of the entire retinas (P <0.01, ANOVA). An additional post-hoc subgroup test was performed to reveal the effects of laser application on GCL nuclei counts, and significant differences were found only at 14 and 21d (Figure 4). Decreases in nuclear density due to cell death were 10.8% at 7d, 30.4% at 14d, and 40.1% at 21d. Investigating cell loss in the GCL, similar post-hoc results were obtained when the peripheral retina and the para-optic retina were separately compared to the equivalent area of the control eye. At 7, 14, and 21d the peripheral retina showed 11.2%, 36.7%, and 39% losses, respectively, while the para-optic retina displayed 10.3%, 25.7%, and 40.2% losses. No significant differences were found between the GCL cell count of the para-optic retinal region and peripheral retina in CRVO eyes (P=0.91, paired t-test).

Cell loss in the BRVO group was evaluated according to three aspects. Firstly, whole retina GCL cell counts were analyzed between the treated eyes and the normal control eyes. Firstly, since there was no significant effect due to time after treatment (P =0.23, ANOVA), data from the three timepoint groups were merged for further comparison. Compared with the contralateral normal control eyes (Figure 5), the ganglion cell number in the BRVO eyes was significantly less (P<0.001, paired t-test). Secondly, different retinal regions (peripheral and para-optic) of the laser treated side were compared, and no significant difference was found in cell counts (P =0.64, paired t-test). Thirdly, comparisons between the laser-treated and the untreated sides of the same eye (Figure 6) revealed no significant difference in ganglion cell number (P=0.47, ANOVA).

The normal rat retina has five well-defined layers in light microscopic views of thin sections: the inner plexiform, the
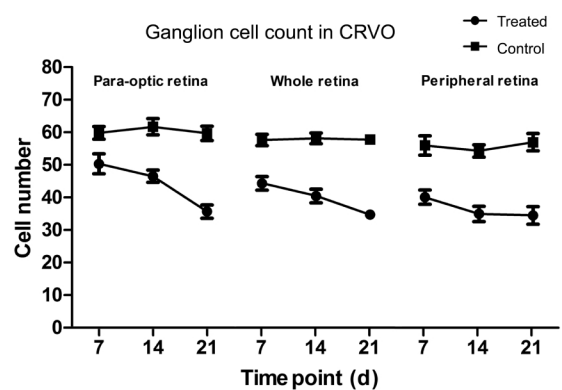
Figure 4 GCL cell count in different retinal areas at different timepoints in the CRVO model.
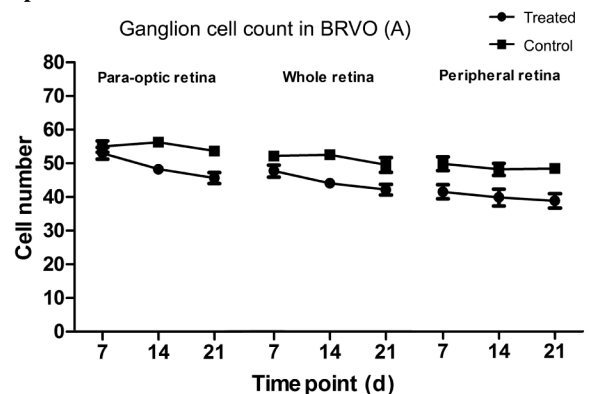
Figure 5 GCL cell count in different retinal areas at different timepoints in the BRVO model: the laser－treated eyes compared with the contralateral eyes.
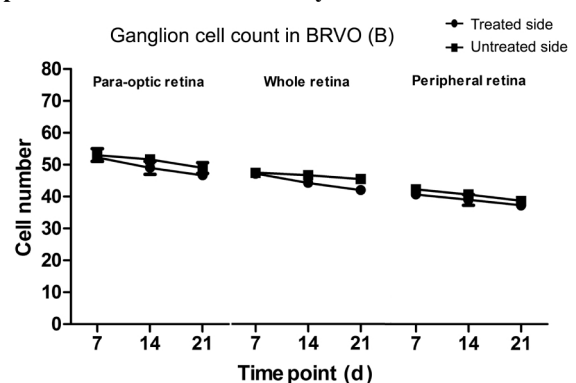
Figure 6 GCL cell count in different retinal areas at different timepoints in the BRVO model: laser－treated side compared with the untreated side of the same eye.
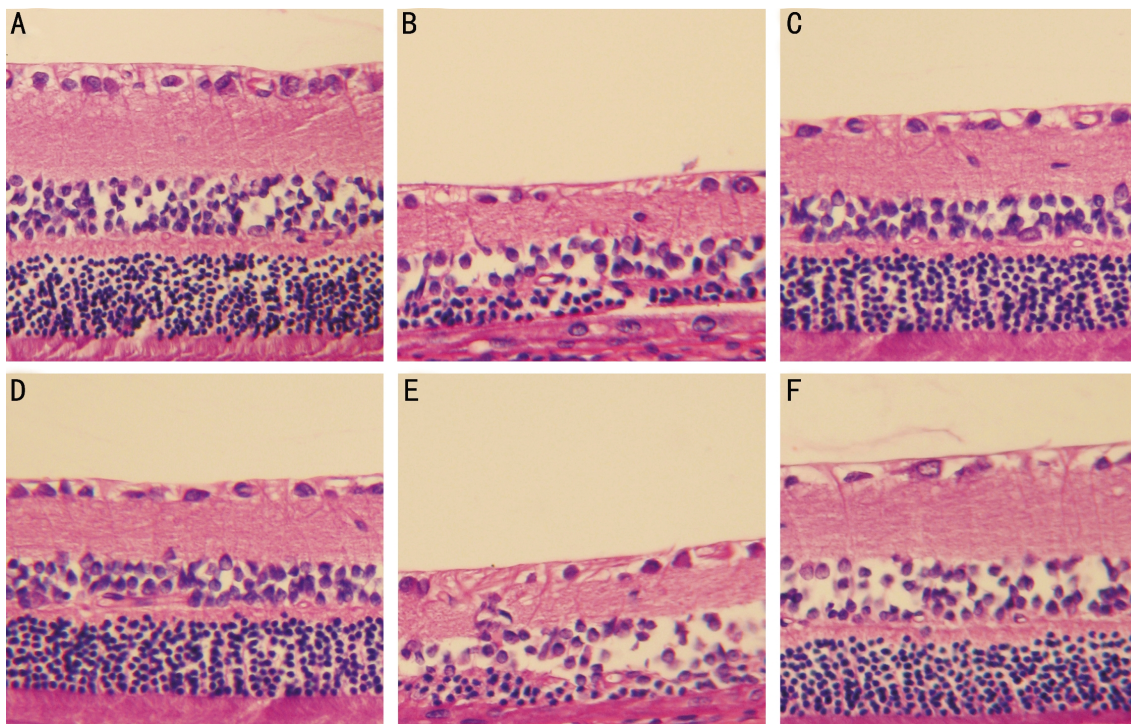
Figure 7 Histopathology of the para−optic and peripheral retinas in CRVO and BRVO rat models at 21d A: Para-optic retina of the control eye; B: Peripheral retina of the control eye; C: Para-optic retina of the CRVO eye: the retinal thickness is remarkably reduced due to the loss of cells; D: Peripheral retina of the CRVO eye; E: Para-optic retina of the BRVO eye; F: Peripheral retina of the BRVO eye.

inner nuclear, the outer plexiform, the outer nuclear, and the GCL (Figure 7). Relative to normal rats, changes in thicknesses of the retinal layers were significant in 21d CRVO rats. There was an obvious decrease in the thickness of the inner retina, which consists of the inner plexiform and inner nuclear layers, and also the GCL. The outer plexiform layer almost disappeared, although this layer is very thin (less than 10 μm) in the normal retina. The most remarkable change appeared in the outer nuclear layer, in which the number of nuclear layers of photoreceptor cells decreased to 2-3 compared with 10-12 in the normal retina.

While changes in thickness could be observed in the para-optic retina of 21d BRVO rats, the severity was less than in CRVO eyes. In contrast with the decreased thicknesses of the inner retinal layers in CRVO rat, changes in the outer nuclear layer were not significant. Unlike the para-optic retina, the peripheral retina appeared to survive well, although the inner nuclear layer became looser.

DISCUSSION

The rat has often been used as a model for studies involving eye diseases, not only because it is relatively inexpensive and easily available, but also because humans and rats share some common features of retinal vasculature architecture. Like humans, rats have two major microvascular networks: a superficial and a deep dense capillary network[11]. This makes the rat an ideal animal model to mimic human retinal vascular diseases, although the rat has no macular area which limits its usefulness for mimicking all the signs typical of human RVO. However, while the course of RVO between humans and rats is not identical, the rat remains the best RVO model and an ideal investigational tool since it is easily handled and the response to treatments is replicable.

Erythrosin B irradiated by laser has previously been used to develop animal models of posterior ischemic optic neuropathy, neuropathic pain, and distal middle cerebral artery occlusion [8-10]. This photothrombotic method of vascular occlusion has gained widespread acceptance as a valid, noninvasive method for producing thrombosis. In the present study, we successfully created a rat RVO model using erythrosin B. In preliminary experiments, we attempted to inject the erythrosin B solution *via* the tail vein, but failed many times. When we chose the dorsal vein of the penis the injection was easily accomplished, since it is superficial and larger than the tail vein. Therefore, rather than using the tail vein, in the present study the erythrosin B solution was injected into the proximal part of the superficial dorsal vein of the penis, in the region of the penile root.

The laser energy used in our study was lower than that reported in several similar RVO animal model studies[6,12-14]. We believe that less laser energy is gentler on the retina and is a better mimic of human RVO. Most human CRVOs are caused by intraluminal thrombus [15]; in our rat model, thrombi were induced by green laser irradiation on target branch veins that were infused with erythrosin B, creating a

histopathology similar to that of human RVO.

Fundus photography and fluorescein angiography recorded a natural course of vein occlusion in both the CRVO and BRVO groups: veins occluded immediately after laser irradiation and were completely reperfused at 7d. The tissue response was similar to that of human RVO, including venous dilatation and tortuosity after occlusion, edema of the entire retina observed one hour after irradiation, remarkable superficial and deep retinal hemorrhages 1d after irradiation, and subsequent gradual regression over time. In some cases of CRVO, yellow precipitates were observed by 21d. These yellow precipitates are presumed to be hemosiderin deposits, an indication of previous retinal hemorrhage[16].

An important characteristic in this model is a temporary marked exudative RD after laser treatment, due to subretinal serous leakage from the damaged microcirculatory system. Serous RD is not common in human CRVO or BRVO, and its occurrence in the rat likely reflects anatomic differences between rodent and primate vascular and retinal architecture. The rate of RD in our experiments was 100%, as in another rat CRVO experiment [17]. In another study, the authors claimed an RD incidence of 25% in their rat models, and speculated that veins irradiated at a spot distance of 1.5-2.0 disk diameters away from the optic nerve may explain the lower rate [7]. However, we did not achieve that outcome despite applying the same method except for a different photosensitizer.

Ocular ischemia ultimately leads to neuronal death. Of the different retinal neurons, retinal ganglion cells are thought to be the most vulnerable to ischemia[18]. In our study, compared with the contralateral control eyes we found significant declines in the densities of nuclei in the GCL of CRVO eyes, while those of the para-optic and peripheral retina were comparable. This result is consistent with what we observed during the course of CRVO course, namely, the edema and hemorrhage of the entire retina. Obvious features observed in the retinas of CRVO patients are inner ischemic atrophy with loss of nerve fiber, ganglion cell, and inner plexiform layers, and loss of the inner aspect of the inner-nuclear layer [19]. Similarly, we found in this CRVO rat model a distinct decrease in the thickness of the inner retina. Such results suggest that our rat CRVO models are similar histologically to human CRVO.

In the BRVO group, the results were similar: significant differences in GCL cell losses between the treated and untreated contralateral eyes, with little or no changes in the para-optic and peripheral retinas. These cell losses suggest that the retinal area surrounding the irradiated spot did suffer from ischemia, and there was no difference in severity of ischemia between para-optic and peripheral retina. In rats of the BRVO group, there was no significant difference in cell loses between the laser-treated and untreated eyes. This suggests a similar pathological course in both sides. It may be that the entire retina was edematous, and the variance with human BRVO could be due to differences in anatomy.

We also found a dramatic decrease in the number of photoreceptor cells in the CRVO model. Photoreceptor apoptosis was previously observed in experimental RD in rats [20]. Thus the bullous RD that occurred in our study may be at least partially responsible for decreases in the cells of the outer nuclear and outer plexiform layers. However, another rat CRVO study without RD also showed visibly fewer cells in the outer nuclear and outer plexiform layers[7]. This evidence suggests that photoreceptor cell loss due to ischemia not only caused RD but also vein occlusion. However, we must note that usually there is no evident atrophy of the outer nuclear and outer plexiform layers in human CRVO, except in cases with concomitant chronic macular detachment. Thus, the major limitation of this model is that the outer retinal disease induced by the irradiation is much more severe than that which occurs in the CRVO patient. This may be associated with the inflammation generated from this model (in addition to ischemia) and the resultant exudative RD. We think this animal model is more suitable for studying RVO with chronic RD.

In summary, herein we demonstrated the development of CRVO and BRVO rat models and their natural history during the initial 21d after irradiation. The model is a possible means of studying the pathogenesis of RVO and evaluating the effects of pharmaceutical treatments.

ACKNOWLEDGEMENTS

REFERENCES

1 Wong TY, Scott IU. Retinal-vein occlusion. *N Engl J Med* 2010;363(22): 2135-2144

2 Kiire CA, Chong NV. Managing retinal vein occlusion. *BMJ* 2012;344: e499

3 Linnèr E. Occlusion of the retinal veins in rabbits induced by light coagulation. *Acta Ophthalmol* 1961;39(4):739-740

4 Takei K, Sato T, Nonoyama T, Miyauchi T, Goto K, Hommura S. A new model of transient complete obstruction of retinal vessels induced by endothelin-1 injection into the posterior vitreous body in rabbits. *Graefes Arch Clin Exp Ophthalmol* 1993;231(8):476-481

5 Hayashi A, Imai K, Kim HC, de Juan Jr E. Activation of protein tyrosine phosphorylation after retinal branch vein occlusion in cats. *Invest Ophthalmol Vis Sci* 1997;38(2):372-380

6 Drechsler F, Köferl P, Hollborn M, Wiedemann P, Bringmann A, Kohen

L, Rehak M. Effect of intravitreal anti-vascular endothelial growth factor treatment on the retinal gene expression in acute experimental central retinal vein occlusion. *Ophthalmic Res* 2012;47(3):157–162

7 Zhang Y, Fortune B, Atchaneeyasakul L-o, McFarland T, Mose K, Wallace P, Main J, Wilson D, Appukuttan B, Stout JT. Natural history and histology in a rat model of laser-induced photothrombotic retinal vein occlusion. *Curr Eye Res* 2008;33(4):365–376

8 Wang Y, Brown DP Jr, Duan Y, Kong W, Watson BD, Goldberg JL. A novel rodent model of posterior ischemic optic neuropathy. *JAMA Ophthalmol* 2013;131(2):194–204

9 Dominguez CA, Kouya PF, Wu WP, Hao JX, Xu XJ, Wiesenfeld-Hallin Z. Sex differences in the development of localized and spread mechanical hypersensitivity in rats after injury to the infraorbital or sciatic nerves to create a model for neuropathic pain. *Gend Med* 2009;6 Suppl 2:225–234

10 DeFazio RA, Levy S, Morales CL, Levy RV, Lin HW, Abaffy T, Dave KR, Watson BD, Perez-Pinzon MA, Ohanna V. A protocol for characterizing the impact of collateral flow after distal middle cerebral artery occlusion. *Transl Stroke Res* 2011;2(1):112–127

11 Yamakawa K, Ahmed Bhutto I, Lu Z, Watanabe Y, Amemiya T. Retinal vascular changes in rats with inherited hypercholesterolemia-corrosion cast demonstration. *Curr Eye Res* 2001;22(4):258–265

12 Wang S, Song B, Wu Q. Establishment of pigmented rabbit model of retinal vein occlusion by excitation of Rose Bengal with double-frequency laser (532nm). *J Shanghai Jiaotong University (Medical Science)* 2011;31 (8):1082–1085

13 Rehak M, Drechsler F, Köferl P, Hollborn M, Wiedemann P, Bringmann A, Kohen L. Effects of intravitreal triamcinolone acetonide on retinal gene expression in a rat model of central retinal vein occlusion. *Graefes Arch Clin Exp Ophthalmol* 2011;249(8):1175–1183

14 Zhang H, Sonoda KH, Qiao H, Oshima T, Hisatomi T, Ishibashi T. Development of a new mouse model of branch retinal vein occlusion and retinal neovascularization. *Jpn J Ophthalmol* 2007;51(4):251–257

15 Green WR, Chan CC, Hutchins GM, Terry JM. Central retinal vein occlusion: a prospective histopathologic study of 29 eyes in 28 cases. *Retina* 2005;25(5):27–55

16 Gilliland MG, Folberg R, Hayreh SS. Age of retinal hemorrhages by iron detection: an animal model. *Am J Forensic Med Pathol* 2005;26(1):1–4

17 Saito Y, Park L, Skolik SA, Alfaro DV, Chaudhry NA, Barnstable CJ, Liggett PE. Experimental preretinal neovascularization by laser-induced venous thrombosis in rats. *Curr Eye Res* 1997;16(1):26–33

18 Hayreh SS, Zimmerman MB, Kimura A, Sanon A. Central retinal artery occlusion: retinal survival time. *Exp Eye Res* 2004;78(3):723–736

19 Green WR, Chan CC, Hutchins G, Terry J. Central retinal vein occlusion: a prospective histopathologic study of 29 eyes in 28 cases. *Trans Am Ophthalmol Soc* 1981;79:371–422

20 Hisatomi T, Sakamoto T, Goto Y, Yamanaka I, Oshima Y, Hata Y, Ishibashi T, Inomata H, Susin SA, Kroemer G. Critical role of photoreceptor apoptosis in functional damage after retinal detachment. *Curr Eye Res* 2002;24(3):161–172